SYNTHESIS OF CE-DOPED ZNS NANOPARTICLES BY CHEMICAL PRECIPITATION METHOD AND INVESTIGATION OF THEIR STRUCTURAL, OPTICAL AND PHOTOVOLTAIC PROPERTIES

M. GUNBAT[a], S. HOROZ[b,*], O. SAHIN[c], A. EKINCI[d]
[a]*Institute of Science and Technology, Siirt University, Siirt, 56100, Turkey*
[b]*Department of Electrical and Electronics Engineering, Faculty of Engineering, Siirt University, Siirt, 56100, Turkey*
[c]*Department of Chemical Engineering, Faculty of Engineering, Siirt University, Siirt, 56100, Turkey*
[d]*Department of Occupational Health and Safety, School of Health, Siirt University, 56100 Siirt, Turkey*

The synthesized Ce-doped ZnS nanoparticles by chemical precipitation method were dropped on TiO_2 coated on FTO conductive glass substrates. The photovoltaic property of the obtained Ce-doped ZnS/ TiO_2/ FTO structure was investigated by measuring current density (J) – voltage (V) and incident photon to current efficiency (IPCE), respectively. Power conversion efficiency of nanoparticles was calculated using the recorded J-V curve. Thus, both IPCE and J-V measurements have been shown experimentally that Ce-doped ZnS nanoparticles can be used as promising sensitizers in photovoltaic applications. Morever, the structural, elemental and photovoltaic properties of Ce-doped nanoparticles were studied by x-ray diffraction (XRD), energy dispersive x-ray (EDX), optical absorption and photoluminescence (PL) measurements, respectively. The characterization results were discussed.

1. Introduction

One of the recent active research topics is the examination of semiconductor nanoparticle materials [1-2]. Semiconductor nanoparticles have their own electrical, optical, and magnetic properties due to quantum confinement and surface effects. These features enable nanoparticles to be used in different applications such as electronics, optics, catalysis and biology [3-5].

One of the alternative approaches to improve the optical properties of nanoparticles is the doping. The optical and electrical properties of the doped nanoparticles have been of great interest to researchers because they can be modified. Both the emission band of the host material and the emission band that can occur due to the additive material are affected by the quantum confinement [6-9].

As is known, rare elements are used as dopants to improve the luminescence properties of nanoparticles because they have the special 4f-4f intra shell transitions [10]. Electroluminescence devices, photonic, biophotonic and optical memory devices are some of the applications of rare-element-doped semiconductor nanoparticles [11].

Especially, the synthesis and characterization of rare-element-doped II-VI semiconductor nanoparticles has received a great deal of attention because of its advantages such as high quantum efficiency and short lifetime [12-13]. Bharvaga et al. [14] has published one of the most important studies on the doped II-VI semiconductor nanoparticles. They reported that doped ZnS nanoparticles show different luminescence. They also suggested doped ZnS nanoparticles can be used in efficient phosphor materials production. In different studies [15-17], different rare-elements doped ZnS nanoparticles were synthesized and their optical properties were investigated.

---

*Corresponding author: sabithoroz@siirt.edu.tr

The recorded result have indicated that these nanoparticles have potential to be used as luminescent materials.

In this present study, Ce, is one of rare- elements, was used as a dopant to synthesize Ce doped ZnS nanoparticles by chemical precipitation method at room temperature. Structural, elemental and optical properties of synthesized Ce-doped ZnS nanoparticles were investigated by x-ray diffraction (XRD), energy dispersive x-ray (EDX), optical absorption and photoluminescence (PL) measurements, respectively. Ce doped $ZnS/TiO_2/FTO$ structure was obtained by dropping Ce doped ZnS nanoparticles on TiO_2 coated on FTO conductive glass. Thus the photovoltaic properties of Ce doped ZnS nanoparticles were investigated by measuring current density (J) – voltage (V) and incident photon to current efficiency (IPCE), respectively. Moreover, power conversion efficiency of Ce doped $ZnS/TiO_2/FTO$ structure was calculated using the recorded J-V curve.

2. Experimental details and characterization

Ce-doped ZnS nanoparticles were synthesized using chemical precipitation technique, which is both feasible and cost-effective. Synthesis process was carried out at room temperature. Steps followed for the synthesis of Ce-doped ZnS nanoparticles;

(1)   0.1 M zinc acetate and 0.00025 M cerium acetate were dissolved in 100 ml of deionized water.

(2)   100 ml of 0.1 M sodium sulfide aqueous solution were poured onto (Zn+Ce) mixture by dropwise.

(3)   Stirring was continued until a homogeneous mixture was obtained. The stirring was then terminated to allow precipitation of the mixture.

(4)   The precipitated sample was removed from the solvent using filter paper.

(5)   The sample on the filter paper was washed several times with distilled water and ethanol, respectively.

(6)   Finally, the wet sample was dried at certain temperature in the oven.

Structural properties of pure ZnS and Ce-doped ZnS nanoparticles were characterized by X-ray diffraction (XRD) on a Rigaku x-ray diffractometer with Cu Kα (λ= 154,059 pm) radiation. Energy dispersive x-ray (EDX) (JEOL JSM 5800) was used to study the elemental analysis of nanoparticles. Optical characterizations were performed by ultraviolet-visible (UV-Vis) and photoluminescence (PL) spectroscopies on a Perkin-Elmer Lambda 2 and a Perkin-Elmer LS 50B, respectively. The incident photon-to-current efficiency (IPCE) and current density (J)- voltage (V) measurements were carried out using PCE-S20 with a monochromatic light source consisting of a 150 W Xe lamp and a monochromator.

3. Results and discussions

The comparison of XRD diffraction patterns of pure ZnS and Ce-doped ZnS nanoparticles is shown in Fig. 1 (a-b), respectively.
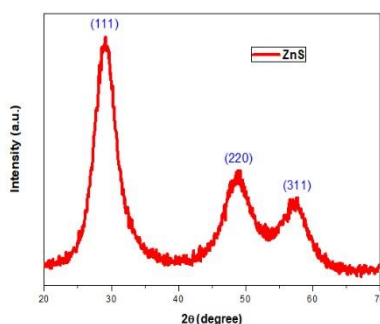
Fig. 1a. The recorded XRD patterns for pure ZnS nanoparticles
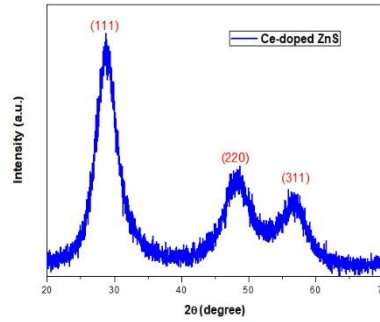
Fig. 1b. The recorded XRD patterns for Ce-doped ZnS nanoparticles

The JCPDS powder difraction file No. 5-0566 reports that ZnS has a zinc blende (ZB) structure which is one of commonly available phases of ZnS. Three diffraction patterns corresponding to (111), (220) and (311) Miller indices were observed at $2\theta = 28.3^0$, 47.6^0 and 56.2^0 values for Ce-doped ZnS nanoparticles. These three diffraction patterns are an indication that the synthesized Ce-doped ZnS nanoparticles are in the cubic structure. Thus, the obtained result is consistent with the JCPDS powder difraction file No. 5-0566. Using the Bragg's relation given in Equation 1, the distance between successive lattice planes of pure ZnS and Ce-doped ZnS nanoparticles was calculated as 0,311 nm and 0.307 nm for (111) plane, respectively.

$$d_{hkl} = \frac{\lambda}{2sin\theta} \tag{1}$$

where, d_{hkl}: interplanar distance, λ: wavelength of x-ray, θ: Bragg's angle.

The calculated values are in a good agreement with observation was reported by Gao et al. [18]. It is possible to calculate the particle sizes of the synthesized nanoparticles using the recorded XRD diffraction patterns with the Scherrer's relation given in Equation (2).

$$t = \frac{k*\lambda}{\beta*cos\theta} \tag{2}$$

where, t: crystal size of nanoparticles, λ: wavelength of x-ray, θ: Bragg's angle, k: constant (its value is 0.9), β: value of full width at half maximum (FWHM).

The calcualted particle size for pure ZnS and Ce-doped ZnS nanoparticles are 2.23 and 2.27 nm respectively. As a result, two important observations should be noted. First, the Ce dopant does not change the crystal structure of ZnS. This is an indication that Ce-doped ZnS nanoparticles were succesfully synthesized. Secondly, the particle size of Ce-doped ZnS nanoparticles is higher than that of pure ZnS due to the Ce dopant. The reason for this is attributed to the ionic radius of Zn^{2+} (88 pm) being smaller than Ce^{3+} (103 pm).

The UV-Vis absorption spectra recorded for pure ZnS and Ce-doped ZnS nanoparticles as a result of optical absorption measurements are shown in Fig. 2 (a-b), respectively.
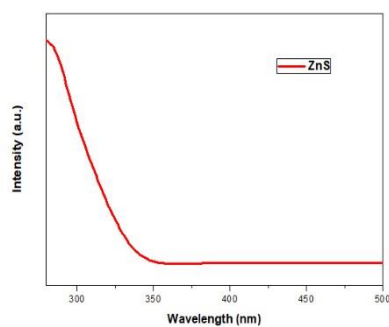
Fig. 2a. The recorded optical absorption spectra for pure ZnS nanoparticles
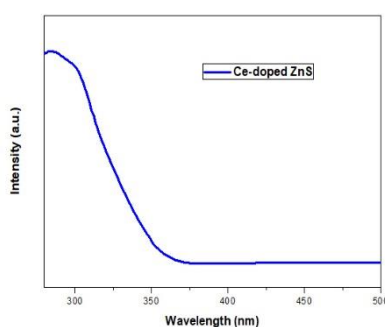
Fig. 2b. The recorded optical absorption spectra for Ce-doped ZnS nanoparticles

Absorption spectrum of pure ZnS nanoparticles was observed at shorter wavelengths than bulk ZnS. This shift, called blueshift, can be attributed to the quantum confinement effect of ZnS nanoparticles [19-20]. Absorption spectra of Ce-doped ZnS nanoparticles were recorded at longer wavelengths than pure ZnS. The similar result was reported by Anand et al. [21]. They explained that Ce might be covalently bonded to ZnS. In addition, this shows that the energy band gap of Ce-doped ZnS nanoparticles is narrower than that of pure ZnS. In other words, a new energy state can occur at the surface of the energy band gap of ZnS nanoparticles [22]. Using the Tauc equation given in Reference [23], the $(\alpha h\nu)^2$ vs $(h\nu)$ curve shown in Fig. 3 (a-b) for both samples was drawn.
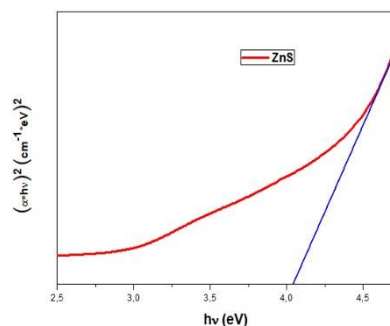
Fig. 3a. The plotted $(\alpha h\nu)^2$ vs $(h\nu)$ curve for pure ZnS nanoparticles
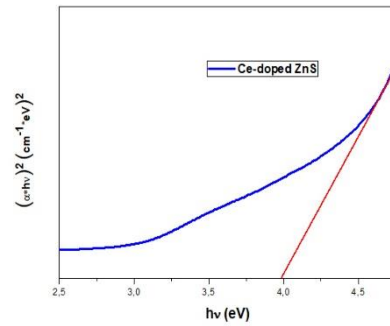
Fig. 3b. The plotted (αhv)² vs (hv) curve for Ce-doped ZnS nanoparticles

Where, α: the absorption coefficient, hv: photon energy. Thus, the energy band gap values of pure ZnS and Ce doped ZnS nanoparticles were determined as 4.04 and 3.97 eV, respectively. Considering the quantum confinement effect, it is expected that the particle size of Ce-doped ZnS nanoparticles having a narrower energy band gap compared to pure ZnS nanoparticles should be larger. The particle size of pure ZnS and Ce-doped ZnS nanoparticles using Brus equation given in Reference [24] was calculated as 2.45 and 2.42 nm, respectively. This result is in agreement with the values obtained for both samples using Scherrer equation.

The PL spectra recorded at room temperature for pure ZnS and Ce-doped ZnS nanoparticles are shown in Fig. 4(a-b), respectively. The excitation wavelength was used as 310 nm.
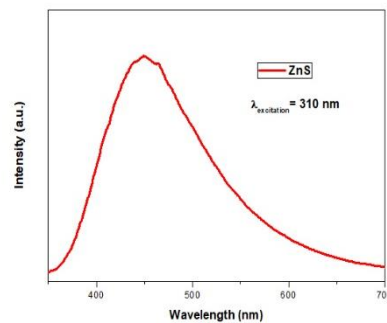
Fig. 4a. The recorded PL spectrum at room temperature for pure ZnS nanoparticles
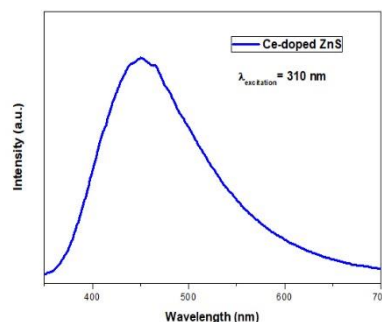
Fig. 4b. The recorded PL spectrum at room temperature for Ce-doped ZnS nanoparticles

A board emission band was observed at 450 and 453 nm for pure ZnS and Ce-doped ZnS nanoparticles, respectively. The peak at 453 nm can be assigned to the presence of surface states owing to Ce dopant while the peak at 450 nm has been attributed to the trap/defect emission of

ZnS. The reason of observed shift in Ce-doped ZnS nanoparitcles could be because of fact that it is difficult to be incorporated Ce^{3+} ions into ZnS lattice since the ionic radius of Zn^{2+} (88 pm) is smaller than that of Ce^{3+} (103 pm). Therefore, Ce^{3+} could be surrounded by ZnS nanoparticles.

EDX measurement was carried out on Ce-doped ZnS nanoparticles to determine if the doping process was successfully performed or not. The EDX spectra recorded for Ce-doped ZnS nanoparticles are shown in Fig. 5. Thus, observing the peaks of the Ce element is an indication that Ce content was successfully doped into ZnS nanoparticles. In addition, the concentrations (%) of Zn, S and Ce elements were determined as 70.142, 29.840 and 0.018, respectively.
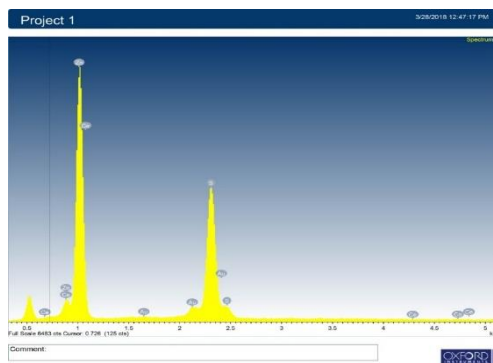
Fig. 5. EDX spectra for Ce-doped ZnS nanoparticles

Photovoltaic properties of synthesized Ce-doped ZnS nanoparticles were investigated in this study for the first time using photon-to-current conversion efficiency (IPCE) measurements. The recorded IPCE spectrum for pure ZnS and Ce-doped ZnS nanoparticles at different incident light wavelengths are shown in Fig. 6 (a-b), respectively.
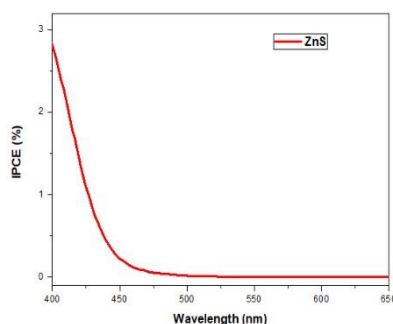
Fig. 6a. The recorded IPCE (%) spectrum at different incident light wavelengths
for pure ZnS/TiO$_2$/FTO Structure
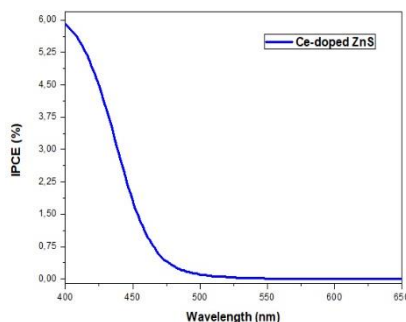
Fig. 6b. The recorded IPCE (%) spectrum at different incident light wavelengths
for Ce doped ZnS/TiO$_2$/FTO structures

Two important observations can be obtained from the Fig. 6 (a-b); (1) Nanoparticles with higher particle size have better IPCE. The recorded IPCE (%) value for Ce-doped ZnS nanoparticles at 400 nm was ~6 while it was 2,8 for the ZnS sample. (2) The spectral response of Ce-doped ZnS nanoparticles is wider than that of ZnS owing to the doping. Due to this feature, more electrons are transferred to the outer circuits and the formation of dark current is suppressed.

Another process for studying photovoltaic properties is to obtain the J-V curves of synthesized nanoparticles. Power conversion efficiency (η) values of pure ZnS and Ce-doped ZnS nanoparticles were calculated using the obtained curves. The J-V curves for pure ZnS and Ce-doped ZnS nanoparticles synthesized on TiO_2 coated on FTO conductive glasses are indicated in Fig. 7 (a-b), respectively.
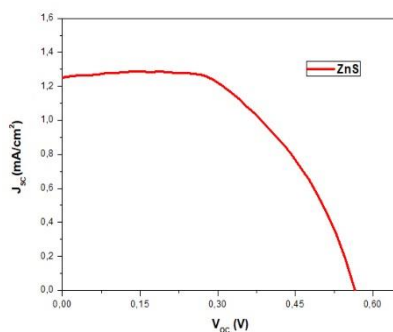
Fig. 7a. Recorded J-V curve for pure ZnS/TiO$_2$/FTO structure
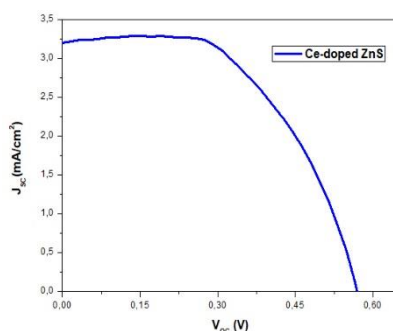
Fig. 7b. Recorded J-V curve for Ce doped ZnS/TiO$_2$/FTO structures

Table 1 shows the η values calculated for both samples using open circuit voltage (V_{OC}) and short circuit current density (J_{SC}) values determined from the curves shown in Fig. 7 (a-b).

Table 1. Values of V_{OC}, J_{SC} and η (%) for pure ZnS/TiO$_2$/FTO and Ce doped ZnS/TiO$_2$/FTO structures

Samples (nanoparticles)	V_{OC} (V)	J_{SC} (mA/cm^2)	η (%)
Pure ZnS/TiO$_2$/FTO	0.56	1.24	2.02
Ce doped ZnS/TiO$_2$/FTO	0,57	3.53	2.27

Taking into account the calculated performance values, Ce dopant seems to be an important factor to boost the efficiency of ZnS-based solar cells. Thus, both IPCE and J-V measurements have been shown experimentally that Ce-doped ZnS nanoparticles can be used as promising sensitizers in photovoltaic applications.

4. Conclusions

The power conversion efficiency ($\eta\%$) for pure $ZnS/TiO_2/FTO$ and Ce doped $ZnS/TiO_2/FTO$ structures was calculated as 2.02 and 2.27, respectively. This result suggests that Ce additive material can play an important role to enhance the efficiency of ZnS-based solar cells. Moreover, it was observed in the IPCE spectra that the spectral response of Ce-doped ZnS nanoparticles is wider than that of ZnS owing to the doping.

Three diffraction patterns observed in the XRD data are an indication that the synthesized Ce-doped ZnS nanoparticles are in the cubic structure. The particle sizes of the synthesized pure ZnS and Ce-doped ZnS nanoparticles using the recorded XRD diffraction patterns were determined as 2.23 and, 2.27 nm, respectively.

The energy band gap values of pure ZnS and Ce doped ZnS nanoparticles were determined as 4.04 and 3.97 eV, respectively. Considering the quantum confinement effect, it is expected that the particle size of Ce-doped ZnS nanoparticles having a narrower energy band gap compared to pure ZnS nanoparticles should be larger.

A board emission band was observed at 450 and 453 nm for pure ZnS and Ce-doped ZnS nanoparticles, respectively. The reason of observed shift in Ce-doped ZnS nanoparitcles could be because of fact that it is difficult to be incorporated Ce^{3+} ions into ZnS lattice since the ionic radius of Zn^{2+} (88 pm) is smaller than that of Ce^{3+} (103 pm). Therefore, Ce^{3+} could be surrounded by ZnS nanoparticles.

Acknowledgements

References

[1] J. Poppe, S. G. Hickey, A. Eychmuller, The Journal of Physical Chemistry C **118**, 17123 (2014).

[2] X. Li, H. Xu, Z.S. Chen, G. Chen, Journal of Nanomaterials **2011**, 1 (2011).

[3] D. Neena, A. H. Shah, K. Deshmukh, H. Ahmad, D. J. Fu, K. K. Kondamareddy, P. Kumar, R. K. Dwivedi, V. Singh, The European Physical Journal D **70**, 53 (2016).

[4] S. Sureh, Applied Nanoscience **4,** 325 (2014).

[5] B. Poornaprakash, S. Ramu, S. H. Park, R. P. Vijayalakshmi, B. K. Reddy, Material Letters **164,** 104 (2016).

[6] R. Kumari, A. Sahai, N. Goswami, Progress in Natural Science: Materials International **25**, 300 015).

[7] D. Saika, J. P. Boroh, Journal of Materials Science: Materials in Electronics **28**, 8029 (2017).

[8] S. Horoz, Superlattices and microstructures **111**, 1043 (2017).

[9] N. P. Huse, A. S. Dive, D. P. Upadhye, S. B. Bagul, K. P. Gattu, R. Sharma, Ferroelectrics **519**, 170 (2017).

[10] V. Kumar, Q. M. Ntwaeaborwa, T. Soga, V. Dutta, H. C. Swart, ACS Photonics **4**, 2613 17).

[11] W. Chen, J. Z. Zhang, A. G. Joly, Journal of Nanoscience and Nanotechnology **4**, 919 (2014).

[12] S. Khajuria, S. Sanotra, H. Kharjuria, A. Singh, H. N. Sheikh, Acta Chimica Slovenia **63**, 104 016).

[13] N. Shanmugan, S. Cholan, G. Viruthagiri, R. Gobi, N. Kannadasan, Applied Nanoscience **4**, 359 (2014).

[14] R. N. Bhargava, D. Gallagher, X. Hong, A. Nurmiko, Physical Review Letters **72**, 416 994).

[15] H. Hu, W. Zhang. Optical Materials **28**, 536 (2006).

[16] P. T. Poojita, V. K. M. S. Rani, U. Chalapthi, M. Kumar, B. Poornaprakash, Chalcogenide

Letters **14**, 11 (2017).

[17] S. C. Qu, W. H. Zhou, F. Q. Liu, N. F. Chen, Z. G. Wang, Applied Physics Letters **80**, 3605 02)

[18] J. Gao, C. Lu, X. Lu, Y. Du, Journal of Materials Chemistry **17**, 4591 (2007).

[19] M. K. Naskar, A. Patra. M. Chatterje, Journal of Colloid and Interface Science **297**, 271 006).

[20] K. Dutta, S. Manna, S. K. De, Synhtetic Metals **159**, 315 (2009).

[21] K. V. Anand, R. Mohan, R. M. Kumar, M. K. Chinnu, R. Joyavel, International Journal of Nanoscience **10,** 487 (2011).

[22] T. Hou, J. Mao, X. Zhu, M. Tu, Rare Metals **25**, 331 (2006).

[23] Z. Q. Mamiyev, N. O. Balayeva, Optical Materials **46**, 522 (2015).

[24] C. Cheng, J. Li, X. Cheng, Journal of Luminescence **188**, 252 (2017).